

Three-dimension (3D) presentation of a hominid cave using ground-penetrating radar

Huthaifa Qawasmeh, Mohammed M. Al-Hameedawi, Lawrence B. Conyers

In **ArchéoSciences** Volume 45-2, Issue 2, July 2021, pages 91 to 95

ISSN 1960-1360

ISBN 9782753586673

This document is the English version of:

Huthaifa Qawasmeh, Mohammed M. Al-Hameedawi, Lawrence B. Conyers, «», ArchéoSciences 2021/2 (No 45-2) , p. 91-95

Available online at:

<https://www.cairn-int.info/journal-archeosciences-2021-2-page-91.htm>

How to cite this article:

Huthaifa Qawasmeh, Mohammed M. Al-Hameedawi, Lawrence B. Conyers, «», ArchéoSciences 2021/2 (No 45-2) , p. 91-95

Electronic distribution by Cairn on behalf of Presses univ. de Rennes.

© Presses univ. de Rennes. All rights reserved for all countries.

Reproducing this article (including by photocopying) is only authorized in accordance with the general terms and conditions of use for the website, or with the general terms and conditions of the license held by your institution, where applicable. Any other reproduction, in full or in part, or storage in a database, in any form and by any means whatsoever is strictly prohibited without the prior written consent of the publisher, except where permitted under French law.



ArcheoSciences
Revue d'archéométrie
45-2 | 2021
Varia

Three-dimension (3D) presentation of a hominid cave using ground-penetrating radar

Huthaifa Qawasmeh, Mohammed M. AL-Hameedawi and Lawrence Conyers



Electronic version

URL: <https://journals.openedition.org/archeosciences/10732>
DOI: 10.4000/archeosciences.10732
ISSN: 2104-3728

Publisher

Presses universitaires de Rennes

Printed version

Date of publication: 31 December 2021
Number of pages: 91-95
ISBN: 978-2-7535-8667-3
ISSN: 1960-1360

Electronic distribution by Cairn



CHERCHER, REPÉRER, AVANCER.

Electronic reference

Huthaifa Qawasmeh, Mohammed M. AL-Hameedawi and Lawrence Conyers, "Three-dimension (3D) presentation of a hominid cave using ground-penetrating radar", *ArcheoSciences* [Online], 45-2 | 2021, Online since 01 December 2021, connection on 13 December 2021. URL: <http://journals.openedition.org/archeosciences/10732> ; DOI: <https://doi.org/10.4000/archeosciences.10732>

Article L.111-1 du Code de la propriété intellectuelle.

Three-dimension (3D) presentation of a hominid cave using ground-penetrating radar

Huthaifa QAWASMEH^a, Mohammed M. AL-HAMEEDAWI^b and Lawrence CONYERS^c

Abstract:

- Determination of the ceiling, floor, and the void of the hominid cave.
- Using time-depth adjustments to correct floor position.
- Statistical method to determine the cave void and real floor depth.
- Creation of a 3D representation for the cave.

Keywords: ground-penetrating radar, 3D presentation, reversal polarity, void measurements cave.

INTRODUCTION

Ground-penetrating radar (GPR) is an active non-invasive method that is typically used to investigate archeological features that are buried in the ground. Here, we employ it in a different environment, which is a fossil-bearing cave in Spain (Bermejo, *et al.* 2020). It is called the Sima del Elefante/Peluda Cave, which is discovered in the late 1800s, when a railroad “trench” was dug in the mountains to make a gently sloping grade for the trains’ tracks in Atapuerca, north of Burgos, Spain. A GPR survey was done in the railroad trench above the Peluda Cave and adjacent to the Sima del Elefante Cave (Bermejo, *et al.* 2020). There has been some success using GPR in caves elsewhere using antenna frequencies between 50–270 MHz range but these surveys typically have had limited resolution (Bermejo, *et al.* 2020; Esmaili, *et al.* 2020; Gosar and Čeru, 2016; Gosar, 2012; and Chamberlain, *et al.* 2000). The antenna frequency used here was 270MHz, which provided a good resolution and up to 6 m depth penetration of energy in the limestone bedrock. A grid of nine GPR profiles was set up,

100 m long and spaced 1 m apart. The time window for data collection was 300 ns with 30 traces/meter (Bermejo, *et al.* 2020). These long profiles were then clipped to 32 m, as only that part of the grid contains the reflections associated with the cave (Fig. 1).

To detect the ceiling/void interface, the first deflection in any trace, which represents the direct ground wave (Fig. 1), was used to determine the normal polarity. All reflections below that first arrival were analyzed and all were of this polarity until a wave was received that represented the reflection from the interface between the limestone ceiling and the void space (Fig. 1). That reflection, which was reversed polarity, was then used to “pick” the same interface in all profiles. The high-amplitude reflection directly below it was then chosen as the floor reflection. Some minor errors in this method occurred in some places where the ceiling/void interface shows a weak normal polarity, which may be due to water saturation contrasts in the limestone rock of the ceiling itself. The radar wave’s velocity as waves are passing through the ceiling rocks is about 0.13 m/ns. When the radar wave then travel in the cave air void, velocity increases

^a Corresponding author, independent researcher, Irbid, Jordan (huth4ifa@gmail.com)

^b General Commission for Groundwater, Ministry of Water Resources, Iraq, PhD student, Department of Geology, University of Baghdad (mohammed-mohsenali@yahoo.com)

^c Department of Anthropology, University of Denver, Denver, Colorado, USA (lawrence.conyers@du.edu)

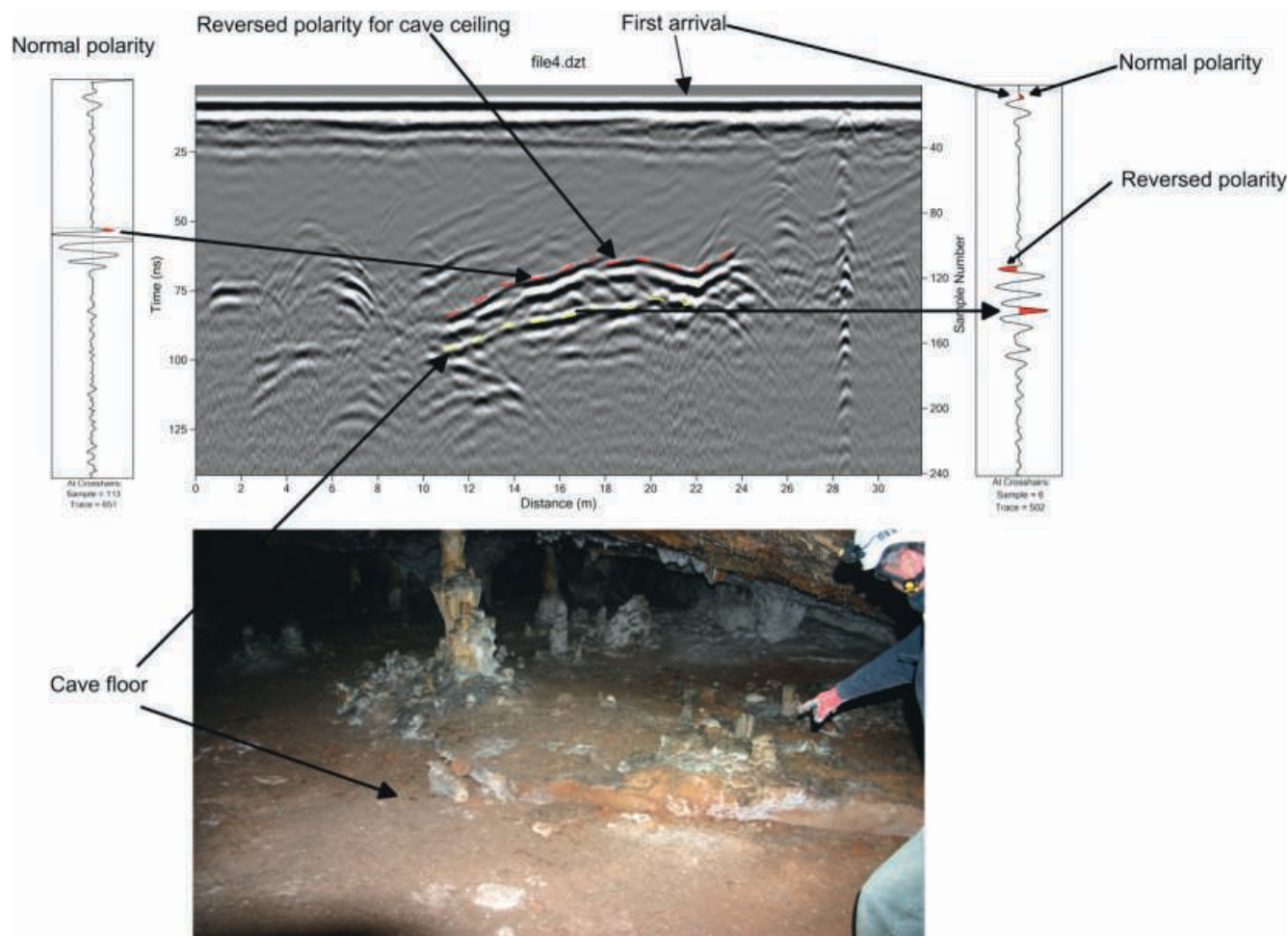


Figure 1: Reflections of the cave on profile 4 and normal and reversed polarity (a), and the cave from inside (b).

to the speed of light (0.3 m/ns). This wave speed-up “pulls up” the reflection of the cave floor (Fig. 1). Bermejo, *et al.* (2020) noted that the void height of the cave appears to be about 1.5 m on the profile shown in Fig. 1, but its actual height is closer to 2.4 m. This discrepancy was adjusted using the speed of light for those waves traveling in the void, placing them in the correct depth position.

3D PRESENTATION OF THE CAVE

For three-dimensional mapping the outline of the cave ceiling and the floor needed to be placed in space, and the digital values of each determined in depth and thickness. The ceiling depth was readily determined as velocity is known and the reflections were “picked” using the phase-following application in ReflexW. Those values were downloaded in two-way travel time (ns) and then converted to a

depth below the ground. The floor-depth computation was a little more problematic due to the air void effect, which speeded up the velocity of the radar wave. Those values were picked in the same way with ReflexW but then adjusted in space as the waves had traveled from the ceiling to the floor and back again in the air.

As an example, in profile 4, this type of adjustment was done in ReflexW by the transformation of the time axis into depth. In this way, the floor location is corrected to its actual position (Fig. 2c), and the resultant ceiling and the floor depth by this method are between 3.9–5.4 m and 6.1–7.2 m respectively. However, the other parts of the profiles are distorted (Fig. 2c). This limitation may cause serious issues when building a 3D representation for underground features. We, therefore, developed a statistical method to calculate the floor depth and place it in its actual position.

This method is based on determining the void height by picking both the ceiling and the floor at the velocity of 0.3

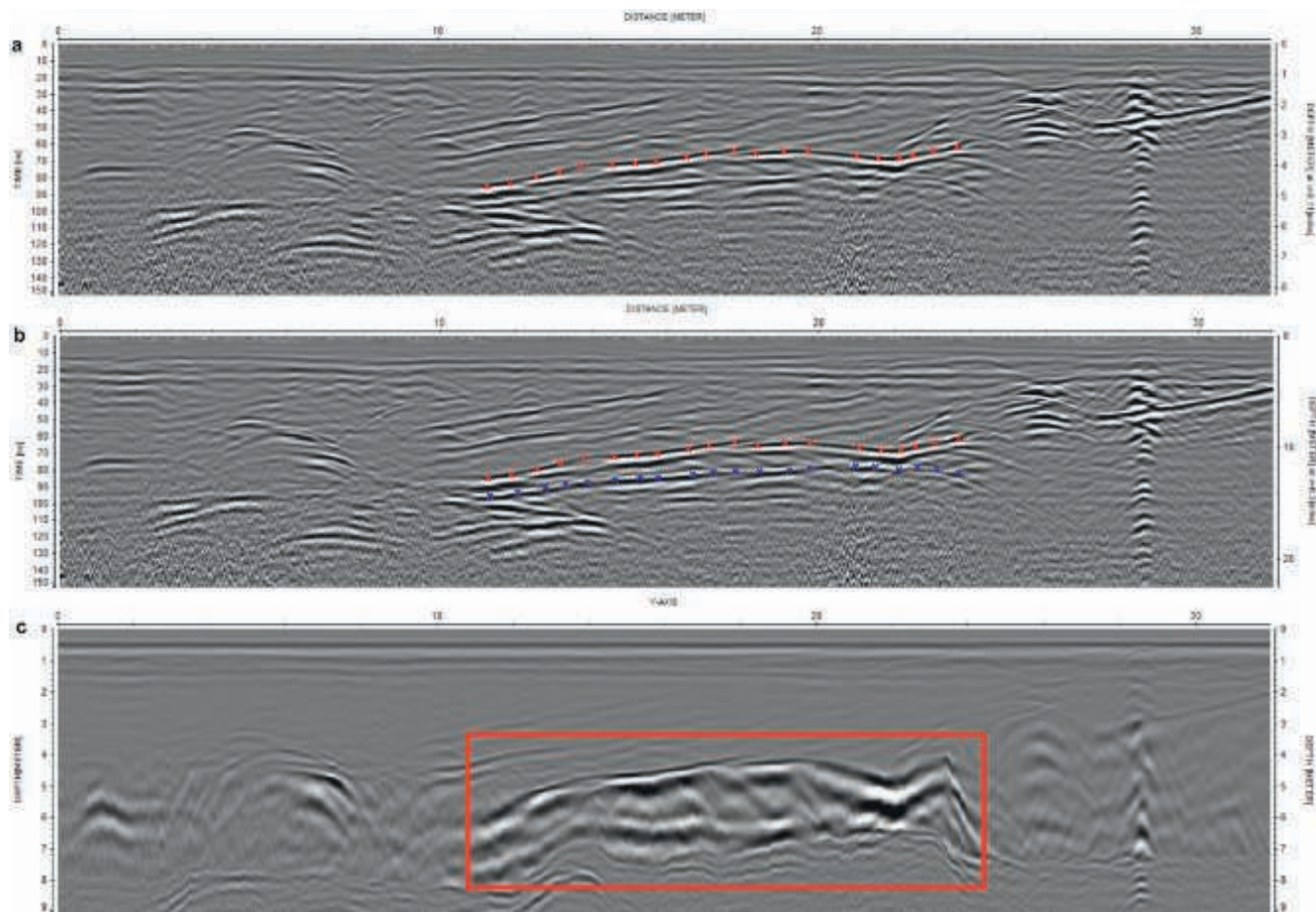


Figure 2: The ceiling picking at the velocity of 0.13 m/ns (a); the ceiling and the floor picking at the velocity of 0.3 m/ns (b); and the time-depth 2D adjustment for the cave reflections (c).

m/ns (the speed of light) using ReflexW software (Fig. 2b). Then subtracting the picking values of the ceiling and the floor by the equation below:

$$vd = fd_{vel0.3} - cd_{vel0.3}$$

Where vd is the void height, cd and fd are the ceiling and floor depth at the velocity of 0.3 m/ns respectively. Then the resultant values of void height (Table 1) should be added to the picking values of the ceiling when the velocity equals 0.13 cm/ns (the velocity of the wave in the cave rocks) (Fig. 2a), to get the actual floor position. This is done by applying the flowing equation:

$$fd_{vel0.13} = vd + cd_{vel0.13}$$

Where vd is the void height, cd and fd are the ceiling depth and the floor depth at the velocity of 0.13 m/ns respectively. The resultant ceiling and floor depth by this method is between 3.9–5.4 m and 6–7.3 m respectively for profile 4 in Fig. 1.

These adjustments were then done to all profiles in the grid after picking and the true depth values of the ceiling

x-axis	y-axis	Ceiling depth	Void height	Floor depth
11.233	3	-5.4801	1.7339	-7.214
11.7	3	-5.3421	1.9462	-7.2883
12.067	3	-5.2195	2.0524	-7.2719
12.533	3	-5.0814	2.2294	-7.3108
12.933	3	-4.9434	2.2294	-7.1728
13.5	3	-4.7288	2.3709	-7.0997
14.033	3	-4.6368	2.5478	-7.1846
14.5	3	-4.6368	2.2647	-6.9015
14.9	3	-4.5908	2.3355	-6.9263
15.4	3	-4.5294	2.4063	-6.9357
15.867	3	-4.4528	2.4063	-6.8591
16.333	3	-4.3607	2.477	-6.8377
16.7	3	-4.2841	2.5479	-6.832
17.233	3	-4.1614	2.7602	-6.9216
17.633	3	-4.0847	2.7955	-6.8802

17.967	3	-4.0387	2.9017	-6.9404
18.4	3	-4.0387	3.0079	-7.0466
18.633	3	-4.1461	2.6539	-6.8
19.1	3	-4.1154	2.6186	-6.734
19.467	3	-4.1154	2.5478	-6.6632
19.9	3	-4.1154	2.2647	-6.3801
20.267	3	-4.1767	-0.1415	-6.3801
20.8	3	-4.2534	1.8754	-6.1288
21.167	3	-4.3147	1.9109	-6.2256
21.567	3	-4.4067	1.6986	-6.1053
22.1	3	-4.4067	1.6632	-6.0699
22.533	3	-4.2534	2.1585	-6.4119
22.967	3	-4.1921	2.194	-6.3861
23.267	3	-4.0694	2.5125	-6.5819
23.6	3	-3.9621	2.8309	-6.793

Table 1: Picking values for the ceiling and the floor at the velocity of 0.13 m/ns and the void height for profile 4.

and the floor were calculated. Those values were imported into Surfer for display (Figure 3). It is be noted that in these procedures the floor reflection displays an uneven surface, which conforms to the actual situation of the cave

that contains many drip features, stalagmites, and ceiling collapse units Figure (1b).

CONCLUSION

Three-dimensional analyses of this sort are especially useful for determining not just a visualization of complex three-dimensional surfaces of this sort, but also for volumetric analysis. Here, the volume of the cave is 185 m³, which is an important value when analyzing air volumes and the origins of this system. The three-dimensional mapping of this complex cave system employed techniques that could easily be applied to any buried features that have distinct tops, bottoms or even sides that can be imaged with GPR. For instance, it could be applied to the top and bottom of shell layers in archaeological deposits, specific layers in complexly bedded tell systems, or any stratigraphic horizons of interest. When the interfaces are “picked” and then measured in three dimensions, outcomes can obtain volumes of units, or images of the buried layers when viewed from multiple directions. Furthermore, it can be used for evaluation and analyzing different subsurface archeological features that contain air volume, such as underground tunnels and passages, and large historical cemetery vaults.

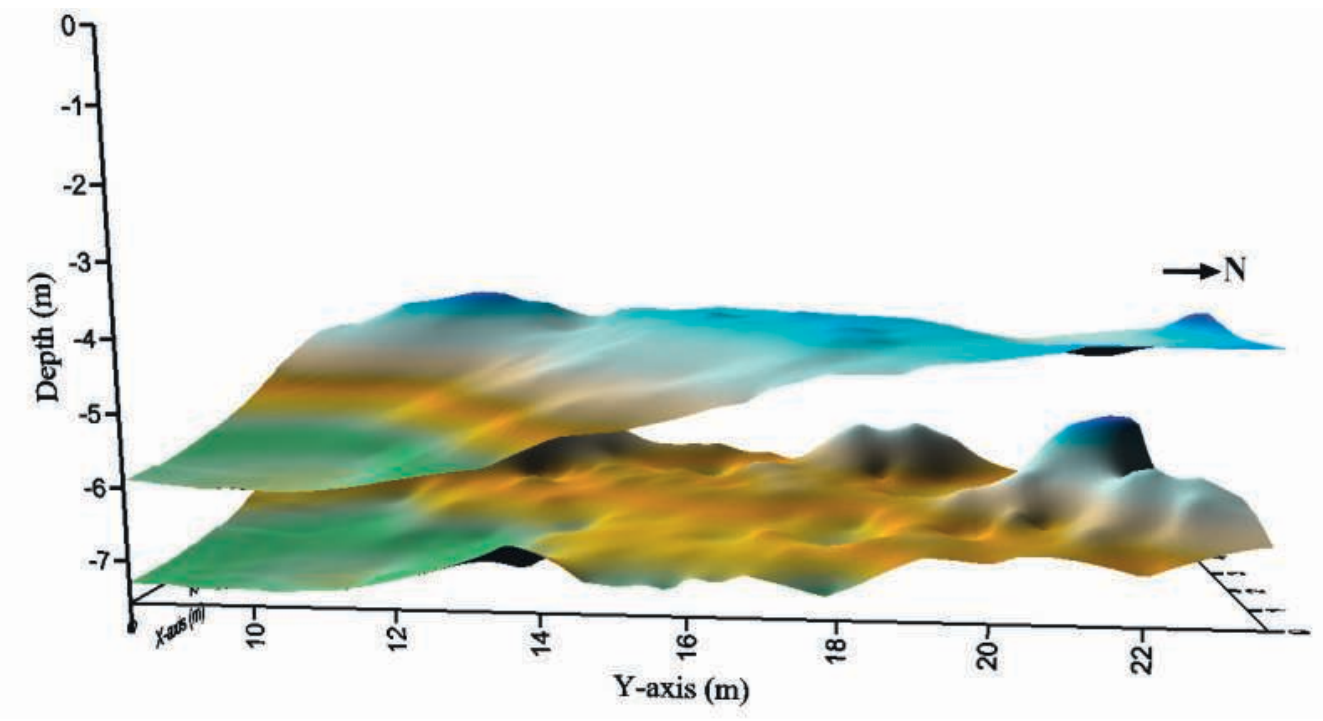


Figure 3: 3D representation of the cave.

References

- Bermejo, L., Ortega, A., I., Parés, J., M., Campaña, I., Bermúdez de Castro, J., M., Carbonell, E., Conyers, L., B., 2020. Karst feature interpretation using ground-penetrating radar: A case study from the Sierra de Atapuerca, Spain. *Geomorphology*, 367.
- Conyers, Lawrence B., 2012. *Interpreting Ground-penetrating Radar for Archaeology*. Routledge, Taylor and Francis Group, New York.
- Chamberlain, A., T., Sellers, W., Proctor, C., Coard, R., 2000. Cave detection in limestone using ground penetrating radar. *Journal of Archaeological Science*, 27: 957–964.
- Esmacili, S., Kruse, S., Jazayeri, S., Whelley, P., Bell, E., Richardson, J., Garry, W. B., and. Young, K., 2020. Resolution of lava tubes with ground penetrating radar: The TubeX project. *Journal of Geophysical Research: Planets*, 23: 1–23.
- Gosar, A., Čeru, T., 2020. Search for an artificially buried karst cave entrance using ground penetrating radar: A successful case of locating the S-19 Cave in the Mt. Kanin Massif (NW Slovenia). *International Journal of Speleology*, 13: 135–147.
- Gosar, A., 2012. Analysis of the capabilities of low frequency ground penetrating radar for cavities detection in rough terrain conditions: The case of Divača Cave, Slovenia. *ACTA CARSOLOGICA*, 41/1: 77-88.